

# Cooperative Zeno shielding in many-body spin systems with long-range interaction: localization and light cone

Lea F. Santos

*Department of Physics, Yeshiva University, New York, New York 10016, USA  
ITAMP, Harvard-Smithsonian Center for Astrophysics, Cambridge, MA 02138, USA*

Fausto Borgonovi and Giuseppe Luca Celardo

*Dipartimento di Matematica e Fisica and ILAMP, Università Cattolica del Sacro Cuore, Brescia, ITALY and  
Istituto Nazionale di Fisica Nucleare, sez. Pavia, Pavia, ITALY*

(Dated: September 28, 2018)

We study the dynamics of many-body quantum spin-1/2 systems with long-range interaction, as the ones recently realized with trapped ions. Our analysis reveals a scenario that is richer than the usual expectation that interactions of longer range should necessarily lead to faster dynamics. Long-range interaction induces superselection rules that become exact in the thermodynamic limit. They confine the dynamics to invariant subspaces, which are shielded from the long-range interaction. Consequently, the evolution may even freeze as the system size increases. We establish an analogy between this effective shielding and the onset of quantum Zeno subspaces, with the difference that here they are driven by system size, instead of interaction strength.

PACS numbers: 75.10.Jm, 03.65.Xp, 67.85.-d

*Introduction.*— A better understanding of the out-of-equilibrium dynamics of many-body quantum systems is central to a variety of fields, from atomic, molecular, and condensed matter physics to quantum information and cosmology. The description of how the initial states of these systems decay in time and how correlations build up can assist in the identification of collective behaviors generated by interactions. New insights into the subject have recently been obtained thanks to the remarkable level of controllability and isolation of experiments with cold atoms and molecules in optical lattices [1–7]. However, most of these experiments have addressed systems with short-range and dipolar interactions. The nonequilibrium dynamics of systems with long-range interaction has been less explored. Long-range interaction arises in many realistic systems, such as cold atomic clouds [8], natural light-harvesting complexes [9, 10], and ion traps [11, 12].

According to the usual definition [13], which is followed in this work, the interaction in a  $d$ -dimensional system is short range, when the coupling strength, decreasing as  $1/r^\alpha$ , has  $\alpha > d$  (in lattice systems,  $r$  is the distance between two sites). Long-range interaction, on the other hand, occurs when  $\alpha \leq d$ . For the latter, a major topic of interest is whether the Lieb-Robinson bound and therefore locality may be violated [14–18]. Experimentally, this point has been investigated with trapped ions [11, 12], where one-dimensional (1D) spin-1/2 systems with  $0 \leq \alpha \leq 3$  were implemented. It was observed that for short-range interaction, the dynamics is characterized by a constant maximal velocity and an effective light cone that bounds the propagation of information. As  $\alpha$  decreases, the propagation velocity increases and eventually diverges. For long-range interaction, where  $\alpha < 1$ , the light-cone picture is no longer valid and the propagation of information is nonlocal [17].

Here, we argue that the general view described above is one of the aspects of the systems with long-range interaction, but other behaviors may also be found, making the subject richer

than a first glance conveys. In particular, we show that the system's dynamics can be shielded from long-range interaction, becoming more localized as  $\alpha$  approaches zero and the system size increases. This rather counterintuitive result is caused by the onset of superselection rules that become exact in the thermodynamic limit.

The reasoning is as follows. Consider the total Hamiltonian,  $H = H_0 + V$ , describing a many-body quantum system, where  $H_0$  has one-body terms and possible short-range interactions, while  $V$  involves only long-range interactions. In the experimentally accessible limit of infinite-range (all-to-all) interaction ( $\alpha = 0$ ),  $V$  can be written as a function of a collective variable (such as total magnetization), which splits its spectrum into highly degenerate energy bands, each one defining an eigensubspace. Depending on the values of the parameters of  $H$  and on system size, the band structure can persist also for the total Hamiltonian. In particular, as the system size increases, the energy bands become more separated and better delineated. Consequently, if the initial state is an eigenstate of  $V$ , its evolution remains mainly confined to the eigensubspace of  $V$  to which it originally belonged. The dynamics is thus shielded from long-range interaction, since the only contribution from  $V$  is a global phase to all the states of the eigensubspace. This is a collective effect, because the time scale over which the shielding is effective diverges with system size. If  $H_0$  does not couple the initial state directly to other states of its invariant subspace, the resulting dynamics can be extremely slow.

It is possible to make a parallel between the dynamical superselection rules induced by long-range interaction and the quantum Zeno effect (QZE) caused by continuous measurements. In the latter case, the dynamics of the system remains confined to subspaces tailored by the interaction part of the total Hamiltonian [19–23], the stronger the interaction is, the better defined the subspaces become. Here, instead of interaction strength, our focus is on the role of system size. We show that, due to long-range interaction, invariant subspaces

are generated by increasing the system size, while the interaction strength is kept fixed. For this reason we name the dynamical effects discussed here *cooperative Zeno shielding*.

*Model.*— We consider a 1D spin-1/2 model with  $L$  sites and open boundary conditions described by the Hamiltonian,

$$H = H_0 + V, \quad (1)$$

$$H_0 = \sum_{n=1}^L (\mathcal{B} + h_n) \sigma_n^z + \sum_{n=1}^{L-1} J_z \sigma_n^z \sigma_{n+1}^z,$$

$$V = \sum_{n < m} \frac{J}{|n - m|^\alpha} \sigma_n^x \sigma_m^x.$$

Above,  $\hbar = 1$  and  $\sigma_n^{x,y,z}$  are the Pauli matrices on site  $n$ . The transverse field has a constant component  $\mathcal{B}$  and a random part given by  $h_n$ , where  $h_n \in [-W/2, W/2]$  are random numbers from a uniform distribution. The nearest-neighbor (NN) interaction in the  $z$ -direction may or not be present,  $J_z \geq 0$ , and  $J$  is the strength of the interaction in the  $x$ -direction with  $\alpha$  determining the range of the coupling. We fix  $J = 1$ . The Hamiltonian with a constant field,  $W = 0$ , and without NN interaction,  $J_z = 0$ , corresponds to the model studied in the experiments with trapped ions [11, 12].

In the case of infinite-range interaction,  $\alpha = 0$ , the  $V$ -part of the Hamiltonian conserves the total angular momentum in the  $x$ -direction.  $H$  can then be written in terms of the total  $x$ -magnetization,  $M_x = \sum_{n=1}^L \sigma_n^x/2$ , as

$$H = \sum_{n=1}^L (\mathcal{B} + h_n) \sigma_n^z + \sum_{n=1}^{L-1} J_z \sigma_n^z \sigma_{n+1}^z + 2JM_x^2 - \frac{JL}{2}. \quad (2)$$

The spectrum of  $V$  is divided into energy bands, each one associated with a particular value of the collective quantity  $M_x^2$ . Each band is characterized by the energy  $E_b = 2J(L/2 - b)^2 - JL/2$ , with a fixed value of  $b$ , where  $b = 0, 1, \dots, L/2$ . An energy band contains  $2\binom{L}{b}$  degenerate states if  $b < L/2$  and  $\binom{L}{b}$  states when  $b = L/2$ . For the total Hamiltonian (2), the eigenstates remain separated by energy bands if  $\mathcal{B}, W, J_z \ll J$ . Alternatively, a band structure can be recovered by increasing  $L$ , keeping fixed the other parameters. This happens because the bands of  $V$  become more separated as  $L$  increases, since  $E_{b-1} - E_b = 2J(L - 2b + 1)$ .

*Light Cones.*— In Refs. [11, 12], the acceleration of information transfer and eventual surpassing of the Lieb-Robison bound achieved by decreasing  $\alpha$  was verified for initial states corresponding to eigenstates of  $H_0$ , where each site had a spin either pointing up or down in the  $z$ -direction. Motivated by the special role of the  $x$ -direction in Eq. (2), here we change the focus of attention to initial states with spins aligned along the  $x$ -axis. They are the eigenstates of  $V$  and are denoted by  $|V\rangle$ . In Fig. 1, we show the evolution of the spin polarization,  $\langle \sigma_n^x(t) \rangle$ , for an initial state where all spins point up in  $x$ , except for the spin in the middle of the chain, which points down, so  $M_x = L/2 - 1$  and  $b = 1$ .

We concentrate first on the interplay between  $V$  and  $\mathcal{B}$ , assuming  $W = 0$  and  $J_z = 0$ . Note that the external field does not couple directly states inside a given band of  $V$ , but only

states in neighboring bands. In Fig. 1 (a), where the interaction is dipolar ( $\alpha = 3$ ) and the bands overlap, the light cone is evident. The polarization of each site changes gradually from the middle of the chain to its borders. This is no longer the case when  $\alpha < 1$ , as exemplified in Fig. 1 (b), which shows a frozen dynamics for an extraordinarily long time. This localization of the spin excitations is caused by both combined factors: the long-range interaction that confines the dynamics to one energy band and the absence of direct coupling inside that band.

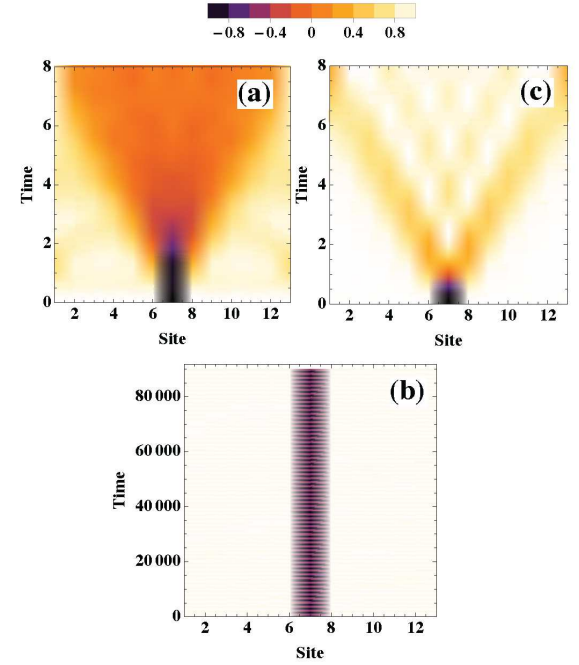


FIG. 1: (Color online) Density plots for the evolution of the polarizations in the  $x$ -direction of all sites of a chain with  $L = 13$  and  $\mathcal{B} = 1/2$ ;  $W = 0$ . Initial state:  $\langle \sigma_7^x(0) \rangle = -1$  and  $\langle \sigma_{n \neq 7}^x(0) \rangle = +1$ . Panel (a):  $J_z = 0$ ,  $\alpha = 3$ ; (b):  $J_z = 0$ ,  $\alpha = 0$ ; (c):  $J_z = 1/2$ ,  $\alpha = 0$ .

By turning on NN interactions,  $J_z \neq 0$ , [Fig. 1 (c)], we witness the reappearance of a light cone. The additional NN interactions directly couple the states  $|V\rangle$  that are inside the same energy band, therefore enabling the evolution of the initial state at short time. Note that for the chosen parameters, the velocities of propagation in Fig. 1 (a) and Fig. 1 (c) are very similar. The appearance of a light cone in the presence of long-range interaction is possible because the initial state considered is effectively shielded from the long-range interaction. We verified that the effects shown in Figs. 1 (b) and (c) occur also for generic long-range interaction ( $0 \leq \alpha \leq 1$ ) [24].

*Quantum Zeno Subspaces.*— Stimulated by the results of Fig. 1, we now fix  $\alpha = 0$  and proceed to a more detailed analysis of the effects of infinite-range interaction and their dependence on system size. For a general treatment, we assume a random transverse field, so  $\mathcal{B} = 0$  and  $h_n \neq 0$ . We take as initial state a random superposition of all states  $|V_k^b\rangle$  that belong to the same band  $b$  chosen for the analysis [25].

In Fig. 2, we compute the probability,  $P_b(t)$ , for the initial state to remain in its original energy band  $b$ ,

$$P_b(t) = \sum_k |\langle V_k^b | e^{-iHt} |\Psi(0)\rangle|^2, \quad (3)$$

where the sum includes all the states of the selected energy band. The results presented are for averages over random realizations and initial states, denoted by  $\langle P_b(t) \rangle$ .

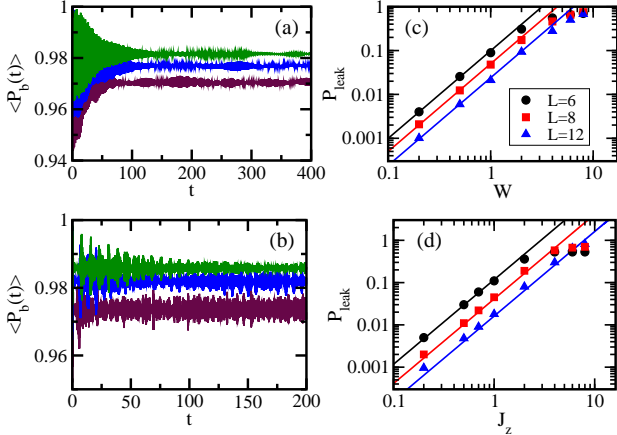


FIG. 2: (Color online) In (a,b):  $\langle P_b(t) \rangle$  for the initial random superposition of states  $|V_k^b\rangle$  from band  $b = 1$  vs time for  $L = 10, 12, 14$  from bottom to top; (a):  $J_z = 0, W = 2$  and (b):  $J_z = 1, W = 0$ . In (c,d):  $P_{\text{leak}}$  vs  $W$  for  $J_z = 0$  (c), and vs  $J_z$  for  $W = 0$  (d). Symbols represent numerical results and full lines, analytical estimates [26] with an overall fitting multiplicative factor. In all panels: averages over 50 realizations,  $\mathcal{B} = 0, \alpha = 0$ .

In Fig. 2, we show the case of  $b = 1$ , but similar results hold for other bands. It is evident from the figure that the probability to remain in the initial band increases with system size. This happens both in the presence of a random transverse field [Fig. 2 (a)] and when NN interactions are added [Fig. 2 (b)]. In the right panels, we plot the asymptotic values of  $P_{\text{leak}} = 1 - \langle P_b(t) \rangle$  as a function of the random field strength for  $J_z = 0$  [Fig. 2 (c)] and vs the NN coupling strength for  $W = 0$  [Fig. 2 (d)].  $P_{\text{leak}}$  represents the probability for  $|\Psi(0)\rangle$  to leak outside its original band. Based on perturbation theory, the estimation of the scaling of the leakage probability with the above parameters is  $P_{\text{leak}} \propto (W/J)^2/L$  in presence of a random field and no NN interaction, and  $P_{\text{leak}} \propto (J_z/J)^2/L$  for NN interaction only [26]. Such scaling relations are consistent with our numerical data, as seen in Figs. 2 (c) and (d). These results show that as the system size increases, the dynamics remains more confined to subspaces where the number of excitations  $b$  is fixed. Note that fixing  $b$  is different from fixing  $M_x$ , since the value of the latter depends on  $L$ .

The invariant subspaces generated by long-range interaction can be related to the quantum Zeno subspaces induced by continuous measurements [19–23]. In the context of the QZE, “continuous measurements” refer to the continuous observations of a system, described by a Hamiltonian  $H_s$ , performed by an “apparatus” characterized by  $gH_{\text{meas}}$ . In the

limit of strong coupling,  $g \rightarrow \infty$ , a superselection rule is induced that splits the Hilbert space into the eigensubspaces of  $H_{\text{meas}}$ . Each one of these invariant quantum Zeno subspaces is characterized by an eigenvalue  $v$  and is formed by the corresponding set of degenerate eigenstates of  $H_{\text{meas}}$ . The dynamics becomes confined to these subspaces and is dictated by the Zeno Hamiltonian  $H_Z = \sum_k \Pi_k H_s \Pi_k + v_k \Pi_k$ , where  $\Pi_k$  are the projectors onto the eigensubspaces of  $H_{\text{meas}}$  corresponding to the eigenvalues  $v_k$ . This scenario has already been studied experimentally [27].

For the system investigated here, we associate  $H_s$  with  $H_0$  and  $gH_{\text{meas}}$  with  $V$ . The subspaces of  $V$  become invariant subspaces of the total Hamiltonian not only when  $J \gg \mathcal{B}, W, J_z$ , which is the scenario of the QZE described above, but also in the large system size limit,  $L \rightarrow \infty$ . The latter is the main focus and the novelty of this work.

When  $J_z = 0$ , the Zeno Hamiltonian coincides with  $V$ , since the transverse field does not couple directly states  $|V_k^b\rangle$  that belong to the same eigensubspace of  $V$ , so  $\sum_k \Pi_k H_0 \Pi_k = 0$ . This explains why the dynamics in Fig. 1 (b) is frozen for very long times. On the other side, in the case where  $\mathcal{B}, W = 0$  and  $J_z \neq 0$ , we can rewrite  $H_0$  in terms of the  $\sigma_n^{\pm x}$  operators that flip the spins in the  $x$ -direction. The projection of the NN part of the Hamiltonian on the eigensubspaces of  $V$  leaves only the term  $\sigma_n^{+x} \sigma_{n+1}^{-x} + \sigma_n^{-x} \sigma_{n+1}^{+x}$ , which leads to a Zeno Hamiltonian with an effective NN interaction that conserves the number of excitations inside each band  $b$ . This explains why in Fig. 1 (c) a typical short-range light-cone appears. The fact that despite the presence of long-range interaction the dynamics can be either frozen or effectively short-ranged is a striking example of the “cooperative Zeno shielding” effect discussed in this Letter.

*Fidelity Decay.*—To substantiate that the dynamics becomes indeed controlled by the Zeno Hamiltonian as  $L$  increases, we analyze the fidelity between an initial state evolved under the total Hamiltonian  $H$  and the same state evolved under  $H_Z$ ,

$$F(t) = |\langle \Psi(0) | e^{iH_Z t} e^{-iHt} | \Psi(0) \rangle|^2. \quad (4)$$

It is clear that if  $H \rightarrow H_Z$  then  $F(t) \rightarrow 1$ . The results are shown in Fig. 3. Equivalently to Fig. 2, we fix  $\mathcal{B} = 0$  and deal with averages over random disorder realizations and over initial states, which gives  $\langle F(t) \rangle$ .  $|\Psi(0)\rangle$  is again a random superposition of all states  $|V_k^b\rangle$  belonging to the same band  $b$ .

In Figs. 3 (a) and (d) the fidelity is plotted vs time for different systems sizes for  $b = 3$ . In panel (a),  $H_0$  contains only the random fields, while in (d),  $H_0$  contains only NN interaction. In both cases the fidelity decay slows down as the system size increases, confirming that  $H_Z$  determines the dynamics for large  $L$ .

When  $H_0$  contains only random fields ( $\mathcal{B}, J_z = 0$ ), since its projection on the  $b$  subspace is zero, the fidelity coincides with the survival probability,  $F(t) = |\langle \Psi(0) | e^{-iHt} | \Psi(0) \rangle|^2 = \left| \sum_{\alpha} |C_{\alpha}^{(0)}|^2 e^{-iE_{\alpha} t} \right|^2$ , where  $C_{\alpha}^{(0)} = \langle \psi_{\alpha} | \Psi(0) \rangle$ ,  $|\psi_{\alpha}\rangle$  are the eigenstates of  $H$ , and  $E_{\alpha}$ , the corresponding eigenvalues. Figure 3 (a) shows that, rather counterintuitively, the dynamics becomes more localized as the system size increases. The onset of invariant subspaces together with the incapability of  $H_0$

to couple states in the same symmetry sector freeze the dynamics as  $L \rightarrow \infty$ .

Note that the survival probability is the Fourier transform of the distribution of  $|C_\alpha^{(0)}|^2$  in energy. We verified that this distribution has a Gaussian form of width  $\omega$ , which results in a Gaussian decay,  $F(t) = \exp(-\omega^2 t^2)$  [28, 29]. As seen in Fig. 3 (a), the agreement between the numerical results and the analytical expression is very good.

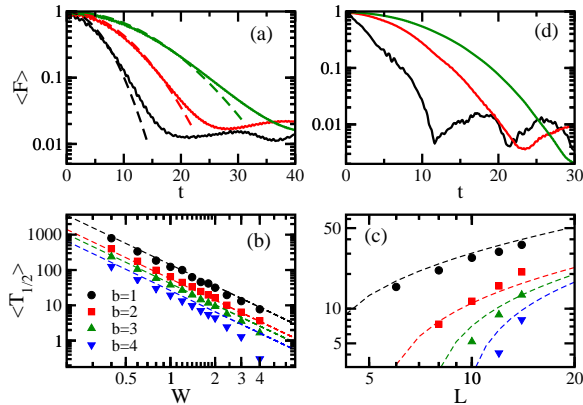


FIG. 3: (Color online) Upper panels: Fidelity decay of  $|\Psi(0)\rangle$  from band  $b = 3$  for  $J_z = 0, W = 2$  (a) and for  $W = 0, J_z = 1$  (d). From bottom to top:  $L = 10, 12, 14$ . Numerical results: full lines. Gaussian expression: dashed lines. Lower panels:  $T_{1/2}$  vs  $W$  for  $L = 12$  (b), and vs  $L$  for  $W = 2$  (c), for  $|\Psi(0)\rangle$  from different bands. In (b,c):  $J_z = 0$ . Numerical data: symbols. Analytical estimate  $T_{1/2} = c_1/\delta E$  with  $c_1$  a fitting parameter: dashed lines. All panels: averages over 50 realizations,  $\alpha = 0, \mathcal{B} = 0$ ; initial states are random superpositions of  $|V_k^b\rangle$ .

In Figs. 3 (b) and (c) we study how the time  $T_{1/2}$  that it takes for the survival probability to reach the value  $1/2$  depends on the disorder strength (b) and on system size (c). Figure 3 (b) provides information associated with the usual QZE, where the quantum Zeno subspaces are induced by decreasing the strength of  $H_0$ . One sees that the dynamics slows down with the decrease of disorder as  $\langle T_{1/2} \rangle \propto W^{-2}$ . In Fig 3 (c),  $\langle T_{1/2} \rangle$  grows with  $L$ , corroborating our claims that the fidelity increases and the excitations become more localized as the system size increases.

We can estimate the dependence of  $T_{1/2}$  on the parameters

of  $H$ . Since the eigenstates of  $V$  in each band are degenerate, the perturbation  $H_0$  mixes them all. In this case, the energy uncertainty  $\omega$  of the initial state can be approximated by the energy spread  $\delta E$  in each band induced by the perturbation. The fidelity decay can then be estimated as  $T_{1/2} \simeq 1/\delta E$ , where  $\delta E$  is computed from perturbation theory (see [26]). For large system sizes one has  $T_{1/2} \propto J\sqrt{L}/W^2$ . The analytical estimates for  $T_{1/2}$  are shown with dashed curves in Figs. 3 (b) and (c). The agreement is very good.

*Conclusion.*— We showed that the presence of long-range interaction can confine the dynamics of the system to invariant subspaces. As  $L$  increases, the evolution of an initial state chosen in one of these subspaces becomes shielded from the long-range interaction. This results in an effective light-cone propagation of information or even the entire freezing of the dynamics.

Notice that our findings do not invalidate previous results associating long-range interaction with the violation of the Lieb-Robinson bound, but instead add new elements to that picture. The analysis of nonequilibrium dynamics can never be detached from the initial state considered. For exactly the same Hamiltonian with long-range interaction, some initial states may lead to a nonlocal propagation of information, as demonstrated experimentally in Refs. [11, 12], while others may be shielded from that interaction, as verified in this work.

A parallel can be drawn between our findings and the quantum Zeno effect. However, the important difference is that here the effect is driven by system size, instead of coupling strength. We conjecture that this is a general feature of long-range-interacting systems, where the long-range part of the Hamiltonian plays a role similar to a measuring apparatus. Long-range interactions can therefore be employed to remove the effects of unwanted terms of the Hamiltonians, providing an additional tool for the control of the dynamics of many-body quantum systems.

## Acknowledgments

We acknowledge useful discussions with F. Izrailev and R. Kaiser. This work was supported by the NSF grant No. DMR-1147430.

---

[1] S. Trotzky, P. Cheinet, S. Fölling, M. Feld, U. Schnorrberger, A. M. Rey, A. Polkovnikov, E. A. Demler, M. D. Lukin, and I. Bloch, *Science* **319**, 295 (2008).  
[2] S. Trotzky, Y.-A. Chen, A. Flesch, I. P. McCulloch, U. Schollwöck, J. Eisert, and I. Bloch, *Nature Phys.* **8**, 325 (2012).  
[3] M. Gring, M. Kuhnert, T. Langen, T. Kitagawa, B. Rauer, M. Schreitl, I. Mazets, D. A. Smith, E. Demler, and J. Schmiedmayer, *Science* **337**, 1318 (2012).  
[4] T. Fukuhara, A. Kantian, M. Endres, M. Cheneau, P. Schausz, S. Hild, D. Bellem, U. Schollwöck, T. Giamarchi, C. Gross, et al., *Nat. Phys.* **9**, 235 (2013).  
[5] K. R. A. Hazzard, B. Gadway, M. Foss-Feig, B. Yan, S. A. Moses, J. P. Covey, N. Y. Yao, M. D. Lukin, J. Ye, D. S. Jin, et al., *Phys. Rev. Lett.* **113**, 195302 (2014).  
[6] T. Langen, R. Geiger, and J. Schmiedmayer, *Annu. Rev. Condens. Matter Phys.* **6**, 201 (2015).  
[7] B. Bauer, T. Schweigler, T. Langen, and J. Schmiedmayer, *arXiv:1504.04288*.  
[8] E. Akkermans, A. Gero, and R. Kaiser, *Phys. Rev. Lett.* **101**, 103602 (2008); R. Kaiser, *J. Mod. Opt.* **56**, 2082 (2009); T. Bieniaime, N. Piovella, and R. Kaiser, *Phys. Rev. Lett.* **108**,

123602 (2012); E. Akkermans and A. Gero, *Euro Phys. Lett.* **101**, 54003 (2013).

[9] J. Grad, G. Hernandez, and S. Mukamel, *Phys. Rev. A* **37**, 3835 (1988); F. C. Spano, J. R. Kuklinski and S. Mukamel, *J. Chem. Phys.* **94**, 7534 (1991).

[10] G. L. Celardo, Paolo Poli, L. Lussardi, and F. Borgonovi *Phys. Rev. B* **90**, 085142 (2014); G. L. Celardo, G. G. Giusteri, and F. Borgonovi *Phys. Rev. B* **90**, 075113 (2014); D. Ferrari, G. L. Celardo, G.P. Berman, R.T. Sayre and F. Borgonovi *Jour. Phys. Chem. C*, **118**, 20 (2014); G. L. Celardo, F. Borgonovi, M. Merkli, V. I. Tsifrinovich and G. P. Berman, *Jour. Phys. Chem. C* **116**, 22105, (2012).

[11] P. Jurcevic, B. P. Lanyon, P. Hauke, C. Hempel, P. Zoller, R. Blatt, and C. F. Roos, *Nature* **511**, 202 (2014).

[12] P. Richerme, Z.-X. Gong, A. Lee, C. Senko, J. Smith, M. Foss-Feig, S. Michalakis, A. V. Gorshkov, and C. Monroe, *Nature* **511**, 198 (2014).

[13] E. A. T. Dauxois, S. Ruffo and M. Wilkens, *Dynamics and Thermodynamics of Systems with Long Range Interactions* (Springer, Berlin, 2002).

[14] M. Hastings and T. Koma, *Comm. Math. Phys.* **265**, 781 (2006).

[15] J. Schachenmayer, B. P. Lanyon, C. F. Roos, and A. J. Daley, *Phys. Rev. X* **3**, 031015 (2013).

[16] J. Eisert, M. van den Worm, S. R. Manmana, and M. Kastner, *Phys. Rev. Lett.* **111**, 260401 (2013).

[17] P. Hauke and L. Tagliacozzo, *Phys. Rev. Lett.* **111**, 207202 (2013).

[18] Z.-X. Gong, M. Foss-Feig, S. Michalakis, and A. V. Gorshkov, *Phys. Rev. Lett.* **113**, 030602 (2014).

[19] A. Peres, *Am. J. Phys.* **48**, 931 (1980).

[20] P. Facchi and S. Pascazio, *Fortschr. Physik* **49**, 941 (2001).

[21] P. Facchi and S. Pascazio, in *Progress in Optics*, edited by E. Wolf (Elsevier, 2001).

[22] P. Facchi and S. Pascazio, *Phys. Rev. Lett.* **89**, 080401 (2002).

[23] P. Facchi and S. Pascazio, in *Proceedings of the XXII Solvay Conference on Physics*, edited by I. Antoniou, V. A. Sadovnichy, and H. Walther (World Scientific, Singapore, 2003).

[24] L. F. Santos, L. Celardo, and F. Borgonovi, (in preparation).

[25] The results for single states  $|V_k^b\rangle$  picked at random from the same energy band are equivalent.

[26] See Supplemental Material.

[27] J. M. Raimond, P. Facchi, B. Peaudecerf, S. Pascazio, C. Sayrin, I. Dotsenko, S. Gleyzes, M. Brune, and S. Haroche, *Phys. Rev. A* **86**, 032120 (2012).

[28] F. M. Izrailev and A. Castañeda-Mendoza, *Phys. Lett. A* **350**, 355 (2006).

[29] E. J. Torres-Herrera and L. F. Santos, *Phys. Rev. A* **89**, 043620 (2014); *Phys. Rev. E* **89**, 062110 (2014); *Phys. Rev. A* **90**, 033623 (2014); AIP Conf. Proc. **1619**, 171 (2014); E. J. Torres-Herrera, M. Vyas, and L. F. Santos, *New J. Phys.* **16**, 063010 (2014).

## Supplementary material for EPAPS

### Cooperative Zeno shielding in many-body spin systems with long-range interaction: localization and light cone

Lea F. Santos<sup>1</sup>, Fausto Borgonovi<sup>2</sup>, and Giuseppe Luca Celardo<sup>2</sup>

<sup>1</sup>*Department of Physics, Yeshiva University, New York, New York 10016, USA*

*ITAMP, Harvard-Smithsonian Center for Astrophysics, Cambridge, MA 02138, USA*

<sup>2</sup>*Dipartimento di Matematica e Fisica and ILAMP, Università Cattolica del Sacro Cuore, Brescia, ITALY*  
*Istituto Nazionale di Fisica Nucleare, sez. Pavia, Pavia, ITALY*

### I. INTRODUCTION TO THE SUPPLEMENTARY MATERIAL

Here, we show how we obtained our estimates for  $P_{\text{leak}}$  and for  $T_{1/2}$ . The first refers to the probability for an initial state  $|V\rangle$ , corresponding to an eigenstate of  $V$ , [see Eq. (1) in the main text] to leak outside its original energy band. The leakage probability is defined as  $P_{\text{leak}} = 1 - \lim_{t \rightarrow \infty} P_b(t)$ , where  $P_b$  is the probability for the initial state to remain in the band  $b$  [see Eq. (3) in the main text].

The time that it takes for the survival probability to reach the value 1/2 is denoted by  $T_{1/2}$ . As discussed in the main text, the survival probability decay shows a Gaussian behavior, which justifies writing  $T_{1/2} \sim 1/\omega$ , where  $\omega$  is the energy uncertainty of the initial state. Since the eigenstates of  $V$  in each band are degenerate, the perturbation  $H_0$  mixes them all. In this case, the energy uncertainty  $\omega$  of the initial state can be approximated by the energy spread  $\delta E$  in each band induced by the perturbation. The analytical expression for the energy

spread  $\delta E$  evaluated at the first nonzero order of perturbation theory is studied below.

The results discussed here are valid in the dilute limit when the number of excitations is small compared to the system size,  $b/L \ll 1$ .

### II. LEAKAGE PROBABILITY

If we start from a certain quantum mechanical state coupled with an amplitude  $\epsilon$  to another quantum mechanical state, the two being separated by an energy  $\Delta$ , the probability to find the system on the second state will never be one, instead, for  $\epsilon/\Delta \ll 1$ , it will be at most of the order  $(\epsilon/\Delta)^2$ . Having this in mind we can estimate the asymptotic value of the leakage probability.

### A. In the presence of an external field and no NN coupling

For the Hamiltonian given by Eq. (2) of the main text, with an external field and no NN coupling ( $J_z = 0$ ), each state  $|V\rangle$  in a band  $b$  is connected to approximatively  $L$  states in the nearest-neighboring bands. The coupling amplitude is  $h_n$ , with  $\langle h_n^2 \rangle = W^2/12$ . Thus, we can define the strength of the coupling as,

$$\epsilon \simeq \frac{W}{\sqrt{12}}.$$

For small  $b$ 's, the energy distance between the neighboring bands is proportional to  $JL$  (see main text), therefore

$$P_{\text{leak}} \propto L \frac{\epsilon^2}{\Delta^2} \propto \frac{W^2}{J^2 L}. \quad (5)$$

As an example, let us consider an initial state  $|V\rangle$  from band  $b = 1$ , where all spins point up in the  $x$ -direction, except for one spin, which points down. The term of the Hamiltonian  $H_0^W$  containing the external field can be written as,

$$H_0^W = \sum_{n=1}^L h_n \sigma_n^z = \sum_{n=1}^L \frac{h_n}{2} (\sigma_n^{+,x} + \sigma_n^{-,x}), \quad (6)$$

where the operators  $\sigma_n^{\pm,x}$  flip the spins pointing in the  $x$ -direction. Due to this term, our initial state is connected with one state in band  $b = 0$  and with  $L - 1$  states in band  $b = 2$ , so that we have:

$$P_{\text{leak}}^{b=1} \simeq \frac{\epsilon^2}{\Delta_{0,1}^2} + (L-1) \frac{\epsilon^2}{\Delta_{1,2}^2},$$

where  $\Delta_{0,1} = 2J(L-1)$  and  $\Delta_{1,2} = 2J(L-3)$  are the energy differences between band  $b = 1$  and the two neighboring bands.

In general, starting with an initial state  $|V\rangle$  in a band  $b$ , there are  $b$  connections with the  $b-1$  band and  $L-b$  connections with the  $b+1$  band, so that

$$P_{\text{leak}}^b \simeq b \frac{\epsilon^2}{\Delta_{b-1,b}^2} + (L-b) \frac{\epsilon^2}{\Delta_{b,b+1}^2}, \quad (7)$$

where  $\Delta_{b-1,b} = E_{b-1} - E_b = 2J(L-2b+1)$ . This expression confirms the general scaling of  $P_{\text{leak}}$  given by Eq. (5).

### B. In the presence of NN coupling and no external field

We can estimate  $P_{\text{leak}}$  also for  $J_z \neq 0$ . The term of  $H_0$  containing the NN interaction can be written as,

$$H_0^{J_z} = \sum_{n=1}^{L-1} J_z \sigma_n^z \sigma_{n+1}^z = \sum_{n=1}^{L-1} \frac{J_z}{4} (\sigma_n^{+,x} + \sigma_n^{-,x})(\sigma_{n+1}^{+,x} + \sigma_{n+1}^{-,x}). \quad (8)$$

In general,  $J_z$  connects a state in band  $b$  with  $m$  states inside that same band,  $n^+$  states in band  $b+2$ , and  $n^-$  states in band

$b-2$ , such that  $m + n^+ + n^- \simeq L$ . For a typical state with  $b$  separated excitations, each one placed at least one site apart from the other, there are  $2b$  states connected in the same band and  $L - 2b - 1$  states connected in the outer bands, so that for  $b/L \ll 1$  the ratio  $n^\pm/m \propto L$ . Since the amplitude of the coupling is  $J_z$ , we can write

$$P_{\text{leak}}^b = \frac{n_+}{m+1} \frac{J_z^2}{\Delta_{b+2,b}^2} + \frac{n_-}{m+1} \frac{J_z^2}{\Delta_{b-2,b}^2} \propto \frac{J_z^2}{J^2 L}$$

Let us compute  $P_{\text{leak}}$  explicitly for the band  $b = 1$ . An initial state  $|V\rangle$  from band  $b = 1$  is coupled to two other states inside that band (apart from the situation where the initial state has an excitation on one of the border sites, 1 or  $L$ , in which case it couples only with one other state) and  $L - 3$  states in band  $b = 3$  (for an excitation on the border we have  $L - 2$  connections), so that we have:

$$P_{\text{leak}}^{b=1} \simeq \frac{(L-3)}{2} \frac{J_z^2}{\Delta_{3,1}^2} = \frac{(L-3)}{8} \frac{J_z^2}{J^2(2L-8)^2}. \quad (9)$$

### III. ENERGY SPREAD

Here, we compute the eigenvalues of the total Hamiltonian given by Eq. (2) of the main text, using second order perturbation theory for degenerate levels. Note that our unperturbed Hamiltonian is the long-range part  $V$ , while we consider  $H_0$  as the perturbation. In the following, we set  $\mathcal{B}, J_z = 0$ , so that the perturbation  $H_0$  is determined only by the random field, as in Eq. (6) above.

Let us consider the energy band  $b = 1$ . We denote the initial state  $|V\rangle$  in this band as  $|1, k\rangle$ , where  $k = 1, \dots, L$  indicates the position of the excitation. In labeling the states, we neglect the double degeneracy due to the flipping of all spins, since the states with  $M_x = (L-2)/2$  are only connected to those with  $M_x = -(L-2)/2$  in a very high order of perturbation theory.

The perturbation  $H_0^W$  [Eq. (6) above] connects the initial state in band  $b = 1$  to the state  $|0, 0\rangle$ , belonging to band  $b = 0$ , and to  $L-1$  states in band  $b = 2$ . The latter states are denoted by  $|2, k, j\rangle$ ; they have one excitation on site  $k = 1, \dots, L-1$  and the other on site  $j = k+1, \dots, L$ , so that the total number of states is  $L(L-1)/2$ .

Since the degeneracy inside the band is not removed at first order of perturbation theory, we use second order perturbation theory for degenerate levels, namely the eigenvalue problem,

$$(V + \epsilon H_0^W) |\psi_1\rangle = (E_1 + \epsilon E_1^I + \epsilon^2 E_1^{II}) |\psi_1\rangle \quad (10)$$

where

$$|\psi_1\rangle = \sum_{k=1}^L c_{0,k} |1, k\rangle + (\epsilon c_{-,0}^I + \epsilon^2 c_{-,0}^{II}) |0, 0\rangle \quad (11) \\ + \sum_{k=1}^{L-1} \sum_{j=k+1}^L (\epsilon c_{+,k,j}^I + \epsilon^2 c_{+,k,j}^{II}) |2, k, j\rangle.$$

The action of the “unperturbed” Hamiltonian on the unperturbed states is trivial,

$$V |b, k\rangle = E_b |b, k\rangle, \quad \text{with } b = 0, 1, 2, \dots$$

while the perturbation  $H_0^W$  acts as,

$$H_0^W|1, k\rangle = h_k|0, 0\rangle + \sum_{j \neq k} h_j|2, k, j\rangle. \quad (12)$$

Collecting the  $\epsilon$  terms in Eq. (10) gives,

$$\begin{aligned} & -E_1^I \sum_{k=1}^L c_{0,k}|1, k\rangle + (E_0 - E_1)c_{-,0}^I|0, 0\rangle + \\ & (E_2 - E_1) \sum_{k=1}^{L-1} \sum_{j=k+1}^L c_{+,k,j}^I|2, k, j\rangle + \\ & \sum_{k=1}^L c_{0,k} \left( h_k|0, 0\rangle + \sum_{j \neq k} h_j|2, k, j\rangle \right) = 0 \end{aligned} \quad (13)$$

Bracketing Eq. (13) respectively with  $\langle 0, 0|$ ,  $\langle 1, s|$  and  $\langle 2, \alpha, \beta|$  with  $\beta > \alpha$ , we obtain,

$$c_{-,0}^I = \frac{1}{E_1 - E_0} \sum_{k=1}^L c_{0,k} h_k, \quad (14)$$

$$E_1^I = 0,$$

$$c_{+, \alpha, \beta}^I = \frac{1}{E_1 - E_2} (c_{0,\alpha} h_\beta + c_{0,\beta} h_\alpha). \quad (15)$$

Collecting the  $\epsilon^2$  terms in Eq. (10) and taking into account that  $E_1^I = 0$ , we have,

$$\begin{aligned} & (E_0 - E_1)c_{-,0}^{II}|0, 0\rangle - E_1^{II} \sum_{k=1}^L c_{0,k}|1, k\rangle + \\ & (E_2 - E_1) \sum_{k=1}^{L-1} \sum_{j=k+1}^L c_{+,k,j}^{II}|2, k, j\rangle + \\ & c_{-,0}^I H_0^W|0, 0\rangle + \sum_{k=1}^{L-1} \sum_{j=k+1}^L c_{+,k,j}^I H_0^W|2, k, j\rangle = 0. \end{aligned} \quad (16)$$

Bracketing Eq. (16) with  $\langle 0, 0|$ ,  $\langle 1, s|$  and  $\langle 2, \alpha, \beta|$  with  $\beta > \alpha$ , we get  $c_{-,0}^{II} = 0$ ,  $c_{+, \alpha, \beta}^{II} = 0$ , and

$$E_1^{II} c_{0,s} = c_{-,0}^I \langle 1, s | H_0^W | 0, 0 \rangle + \sum_{j > k} c_{+,k,j}^I \langle 1, s | H_0^W | 2, k, j \rangle, \quad (17)$$

The equation above, due to the symmetry of the coefficients  $c_{+,k,j}^I = c_{+,j,k}^I$  [see Eq. (15)] can be rewritten as,

$$E_1^{II} c_{0,s} = c_{-,0}^I h_s + \sum_{j \neq s} c_{+,s,j}^I h_j. \quad (18)$$

Inserting Eq. (14) and Eq. (15) in Eq. (18), one finds that the second order corrections  $E_1^{II}$  are the solutions of the  $L$  equations,

$$\begin{aligned} & c_{0,s} \left[ \frac{h_s^2}{(E_1 - E_0)} + \sum_{k \neq s} \frac{h_k^2}{(E_1 - E_2)} - E_1^{II} \right] + \\ & \sum_{j \neq s} c_{0,j} h_s h_j \left[ \frac{1}{(E_1 - E_0)} + \frac{1}{(E_1 - E_2)} \right] = 0, \end{aligned} \quad (19)$$

with  $s = 1, \dots, L$ . In other words,  $E_1^{II}$  are the eigenvalues of the symmetric matrix  $C$ , whose diagonal elements are,

$$C_{ss} = \frac{h_s^2}{(E_1 - E_0)} + \sum_{k \neq s} \frac{h_k^2}{(E_1 - E_2)}, \quad (20)$$

and off-diagonal elements for  $k \neq s$  are,

$$C_{ks} = h_k h_s \left[ \frac{1}{(E_1 - E_0)} + \frac{1}{(E_1 - E_2)} \right]. \quad (21)$$

Let us now estimate the eigenvalues of this matrix in the limit of large  $L$ , at fixed  $W$ . We know that,

$$E_1 - E_0 = 2J(1 - L) \quad \text{and} \quad E_1 - E_2 = 2J(L - 3),$$

therefore, in the limit of large  $L$  one has that the off-diagonal elements are negligible with respect to the diagonal ones, since  $C_{ks} \propto 1/\sqrt{L}$  for  $k \neq s$ , while  $C_{ss} \propto \sqrt{L}$ .

Thus, we can estimate the eigenvalues from the diagonal elements only. In particular, since we are interested in the energy spreading, we evaluate

$$\begin{aligned} \delta E^2 &= \langle C_{ss}^2 \rangle_W - \langle C_{ss} \rangle_W^2 \\ &= \frac{W^4}{180J^2} \left( \frac{1}{(L-1)^2} + \frac{L-1}{(L-3)^2} \right). \end{aligned} \quad (22)$$

where in computing the average over disorder we took into account that

$$\langle h_s h_k \rangle_W = 0 \quad \text{for} \quad s \neq k,$$

and

$$\langle h_s^2 \rangle_W = \frac{W^2}{12}, \quad \text{and} \quad \langle h_s^4 \rangle_W = \frac{W^4}{80}.$$

In the limit of large system size, we therefore get the asymptotic behavior,

$$\delta E \sim \frac{W^2}{J\sqrt{L}}. \quad (23)$$

The generalization to an arbitrary band  $b$  is far from trivial. We will provide the details of this derivation in a longer version of this Letter. We present here only the final result. Similar to the case  $b = 1$ , we can estimate the energy spreading for the general  $b$  band as,

$$\delta E^2 = \frac{W^4}{180J^2} \left( \frac{b}{(2b - L - 1)^2} + \frac{L - b}{(L - 2b - 1)^2} \right).$$

which gives the same estimate as in Eq. (23).